Excess conductivity and pair-breaking effects in $YBa_2Cu_3O_7$ and $Bi_2Sr_2Ca_{1-x}Y_xCu_2O_{8+\delta}$ systems

S. N. Bhatia and C. P. Dhard
Department of Physics, Indian Institute of Technology, Bombay 400 076, India
(Received 27 September 1993)

To explain the behavior of thermal fluctuations, we have measured the electrical resistivity of five samples: thin-film $YBa_2Cu_3O_7$, polycrystalline $YBa_2Cu_3O_7$, and $Bi_2Sr_2Ca_{1-x}Y_xCu_2O_{8+\delta}$ with $x=0$, 0.05, and 0.20. The whole temperature range of fluctuations consists of three regions. Within the mean-field region, $YBa_2Cu_3O_7$ and $Bi_2Sr_2Ca_{1-x}Y_xCu_2O_{8+\delta}$ samples show predominantly three-dimensional (3D) and 2D behaviors with the exponents $\frac{1}{2}$ and 1, in the critical region the two systems display a behavior analogous to 3D-XY and 2D-XY models, respectively. Above the mean-field region [$\ln(\epsilon)\geq -1.0$] exponents have values larger than those predicted by Reggiani *et al.* Both the systems favor strong pair-breaking effects and integral dimensions for the thermal fluctuations.

I. INTRODUCTION

In order to unravel the mechanism of conduction of high-T_c superconducting materials, the study of electrical resistivity has been the subject of intense investigations. In well-oxygenated samples (polycrystalline as well as single crystals) the resistivity drops linearly with temperature and below a so-called on-set temperature deviates from the linear behavior before approaching zero. This depression in resistivity or the enhancement in conductivity is also known as paraconductivity (σ_p) and is affected by fluctuations of small regions of the sample where Cooper pairs are produced. Aslamazov and Larkin[1] (AL) have shown that this excess conductivity in the mean-field approximation to the BCS theory is given by

$$\sigma_{\rm AL}=C_{\rm AL}\epsilon^{-\nu}=\frac{e^2}{32\hbar s}\epsilon^{(D-4)/2} \tag{1}$$

with $\nu=\frac{1}{2}$ and $s=\xi_c(0)$ for the three-dimensional ($D=3$) isotropic conduction and $s=d/2$, $\nu=1$ for thin-film samples where the conduction is restricted within the plane of the film ($D=2$). Here d is the film thickness, $\xi_c(0)$ the amplitude of the coherence length perpendicular to the film plane and $\epsilon=(T-T_c^{\rm mf})/T_c^{\rm mf}$ with $T_c^{\rm mf}$ the mean-field critical temperature. For strongly anisotropic superconductors Lawrence and Doniach[2] (LD) used an anisotropic-mass formulation of the AL theory to derive

$$\sigma_{\rm LD}=\frac{e^2}{16\hbar d\epsilon}\frac{1}{[1+\lambda(\epsilon)]}\ , \tag{2}$$

where $\lambda(\epsilon)=[2\xi_c(\epsilon)/d]^2=(2\alpha/\epsilon)$ with $\alpha=2[\xi_c(0)/d]^2$. This equation predicts a cross over from a 2D ($\sigma_{\rm LD}\simeq 1/\epsilon$) to a 3D ($\sigma_{\rm LD}\simeq 1/\sqrt{\epsilon}$) behavior to occur at a temperature $T_{\rm cr}$ given by

$$T_{\rm cr}=(\{[2\xi_c(0)/d]\}^2+1)T_c^{\rm mf}\ . \tag{3}$$

Anisotropies in the crystal structure of the cuprates affect the transport properties and possibly cause the reduced dimensional nature of conduction in these systems. σ_p is also expected to show a similar behavior. Two factors influence strongly the determination of the dimensionality of σ_p: the procedure used to separate the measured conductivity into the normal (σ_n) and the paraconductivity parts and the determination of the $T_c^{\rm mf}$ to be used in the calculation of σ_p [Eqs. (1) and (2)].

Out of the four families of the oxide superconductors $La_{2-x}Ba_xCuO_4$ (LBCO), $YBa_2Cu_3O_7$ (YBCO), $Bi_2Sr_2CaCu_2O_{8+\delta}$ (BSCCO), $Tl_2Ba_2CaCu_2O_{8+\delta}$ (TBCCO), YBCO has been studied most extensively. In polycrystalline YBCO, it has been possible to fit σ_p to the 3D AL model within the temperature range $-5.0\leq\ln(\epsilon)\leq -2.8$ with an effective $\xi_c(0)$ around 2.0 Å. Above $\ln(\epsilon)\geq -2.0$, σ_p fell rapidly to zero with absence of any 2D region, and was attributed to the predominance of short-wavelength fluctuations falling outside the purview of Ginsburg-Landau (GL) and hence the Al theory.[3] The data on thin films with their c-axis oriented perpendicular to the substrate, agreed well with the LD model within $-5.0\leq\ln(\epsilon)\leq 0.7$ except that a qualitative factor $C=\frac{1}{7}$ had to be introduced to match the magnitude of σ_p with that predicted by the model.[4] Measurements of Hagen, Wang, and Ong[5] on the single crystals agreed well within the 2D AL model but gave a T_c 3–5 K below T_c ($\rho=0$). Friedmann *et al.*[6] from their measurements on the single crystals showed that it was possible to fit both the models mentioned above, even including the Maki-Thomson term[7] (see below) with almost the same precision over very wide temperature range extending to temperatures as high as 200 K. The $T_c^{\rm mf}$ obtained here had no correlation with the inflection point of the resistivity curve or with T_c ($\rho=0$) and the effective correlation length $\xi_c(0)$ and the interlayer spacing d had values too small to be physically meaningful. Veira and Vidal[8] from their extensive studies on polycrystalline samples of YBCO have shown the individual grains in these samples to exhibit σ_p similar to those in single crystals. The factors like C or the unusually small values of $\xi_c(0)$ and d observed in the polycrystalline samples result due to random orientations of the a-b planes of the grains and are accounted for by introducing a temperature-independent factor p which accounts for the reduction of the effective cross-sectional area of the samples due to the various orientations of the a-b planes. In YBCO samples

they find large regions of 3D behavior with a cross over to 2D, whereas the mean-field region in BSCCO to be dominated by 2D behavior only. Later Bhatia *et al.*[9] observed a cross over with a small 3D region in these samples also. It is essential to estimate the σ_n by an independent method. Fitting the data to an expression for the total conductivity containing 5 to 6 adjustable parameters, leads only to an erroneous evaluation of σ_p and therefore, of the parameters involved therein. With σ_p evaluated the next parameter required to analyze σ_p is $T_c^{\rm mf}$. Choosing a criteria for $T_c^{\rm mf}$ is as good as fixing it. In Veira's analysis of YBCO, both choices of $T_c^{\rm mf}$ ($T_{\rm cl}$ and $T_{\rm cr}$) give exponent $\nu=0.48$, corresponding to a 3D AL behavior for YBCO and 0.97 for BSCCO, leaving no room for the inclusion of any other contribution to σ_p. Alternative methods not requiring *a prior* knowledge of $T_c^{\rm mf}$ such as the Testardi plots[10] or the logarithmic derivative plots[11] may prove useful here.

After the decay the quasiparticles of the pair continue to exist in phase locked state for a time τ_ϕ till further collisions destroy this phase relationship. This enhances the conductivity further and this anomalous contribution, calculated by Maki and Thompson[7] (MT) and later modified by Hikami and Larkin[12] has been the subject of recent investigations. The earlier analysis of σ_p completely ignored this contribution. Most of the present efforts to detect this term appear to have been concentrated on YBCO only. Thus Matsuda *et al.*[13] find strong pair-breaking effects ($\tau_\phi \simeq 10^{-14}$ sec) corresponding to negligible conductivity contribution by this effect to their zero-field data of polycrystalline YBCO. Hikita and Suzuki[14] also find similar effects in the monocrystals of YBCO, but they appear to have overestimated σ_p as they find significant value of σ_p to be present even at 200 K ($T \geq 2T_c$). Kim *et al.*[15] in their analysis of YBCO thin films could accommodate a substantial contribution of MT term with $\tau_\phi \simeq 10^{-13}$ sec. Veira and Vidal[16] rule out any important contribution ($\tau_\phi \leq 10^{-14}$ sec) from this effect in YBCO as well as $Bi_{2-x}Pb_xSr_2CaCu_2O_{8+\delta}$ even after allowing the quality of the fit to deteriorate.

It has been proposed that the thermal fluctuations develop in a space having fractal topology. In that case, Char and Kapitulnik[17] have shown the exponent ν to be given by

$$\nu = 2 - \tilde{d}/2 , \tag{4}$$

where $\tilde{d}$ is the fractal dimension of the fluctuations. A deviation in the value of ν from $\frac{1}{2}$ or 1 has been interpreted as the evidence for the presence of the fractals but there is no consistency in these results. Thus Clippe *et al.*[18] obtain integral values for $\tilde{d}$ in ceramic samples of YBCO whereas Pureur *et al.*[11] observe a transition from $\tilde{d}=\frac{4}{3}$ to $\frac{7}{3}$ in same material. In the Bi series the results are equally controvertial. Fractional dimension of $\frac{7}{3}$ has been observed by Clippe *et al.*[18] whereas Mori, Wilson, and Ozaki[19] observed the integral value of 2 in BSCCO.

We have measured the resistivity of five samples: thin-film and polycrystalline YBCO and $Bi_2Sr_2Ca_{1-x}Y_xCu_2O_{8+\delta}$ doped with $x=0$, 0.05, and 0.20 and have analyzed the data in the conventional least-squares fitting procedure as well as by Testardi and the logarithmic derivative plots and find the MT contribution to be present below the detection level in zero field and the fluctuations to grow in integral dimensions as the temperature is reduced towards $T_c^{\rm mf}$.

II. EXPERIMENTAL

YBCO bulk samples were prepared by the solid state reaction method by reacting Y_2O_3, $BaCO_3$ and CuO at 930 °C for 24 hrs. After two intermediate grindings the samples were annealed in the O_2 atmosphere at 900 °C and cooled down to 600 °C at the rate 1 °C/min and maintained at that temperature for 12 hrs. Temperature was further reduced to 300 °C at the rate 0.5 °C/min and then furnace cooled to room temperature. YBCO thin-film samples were grown by the laser ablation technique on $SrTiO_3$ substrate. The BSCCO samples were prepared by matrix precursor method by reacting Bi_2O_3 to $Sr_2CaCu_2O_8$ precursor in the presence of O_2 at 900–950 °C. X-ray diffraction analysis confirmed the polycrystalline samples to be of single phase and films to be aligned with c axis perpendicular to the substrate surface. dc resistivity measurements were performed on the bar shaped samples ($1\times2\times8$ mm^3) by the standard four probe method. Current leads were fixed on the side faces of the bars with Ag paste curing at 100 °C (approx.). On the films, pads were deposited by silver evaporation, and then Ag wires were attached with the paste. Current density used was typically 0.1 A/cm^2, which is much less than the critical current density in bulk. Keithley 224 programmable current source and 181 Nanovoltmeter were used as current source and voltage measuring device. The sample temperature was measured by a calibrated Si diode (LakeShore DT500 recalibrated against Pt thermometer) which was in contact with the sample in a Cu sample holder. The temperature was controlled by LakeShore DRC-91C temperature controller. The sample temperature was lowered with the cooling rate $\simeq 0.5$ K/hr and the data were taken at the interval of 10 mK within the critical and mean-field regions and 0.5 K in the normal region.

III. RESULTS AND DISCUSSION

The resistivity of all the five samples—thin-film and polycrystalline YBCO and the three samples of BSCCO—decreases linearly with temperature thereby showing a metallic behavior in the normal state. The width of the transition for both types of samples is around 1 K. Upon numerically differentiating the data by linear least-squares fitting three points in a walking window, the $d\rho_T/dT$ obtained showed temperature-independent straight line in the normal state region ($T \geq 2T_c$) and a single peak in the transition region which shows the samples to consist of single phase only. The behavior of YBCO in the transition region is shown in Fig. 1. Similar behavior has been found in other samples also.

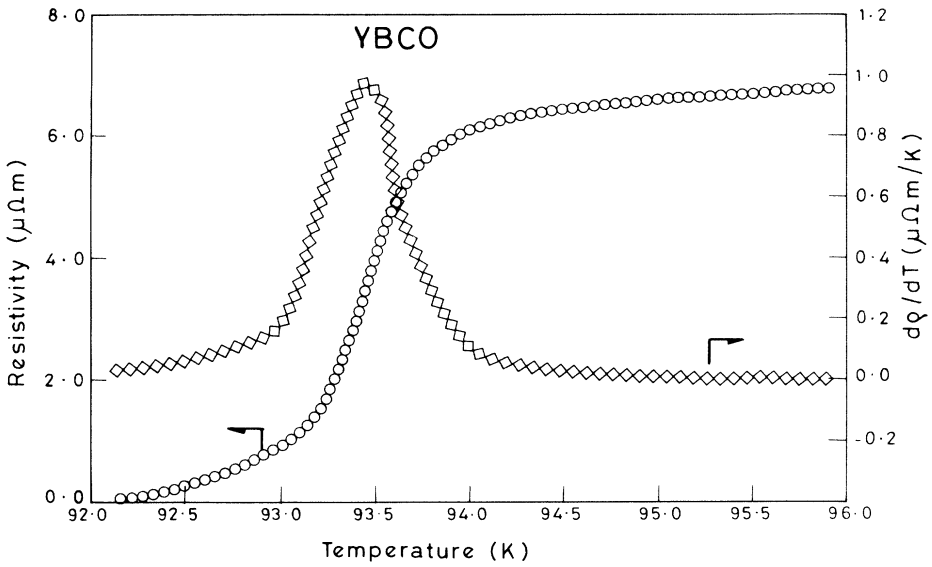

FIG. 1. Experimental resistivity (circles) and its temperature derivative (squares) plotted against temperature in the transition region for the YBCO polycrystalline sample. Single symmetric $d\rho_T/dT$ peak shows the sample to be of single phase.

A. Background conductivity fittings

Data in the normal state were fitted to the expression proposed by Veira and Vidal[8]

$$\rho_B = \rho_{gB}/p + \rho_c \ , \tag{5}$$

where ρ_{gB} is the normal state resistivity of an individual grain, p averages the inclinations of the a-b planes of individual grains to the direction of the current flow and ρ_c gives the intergrain resistivity. ρ_{gB} has been observed to follow either the linear metallic $[\rho_{gB}(L) = A + BT]$ or the Anderson-Zou (AZ) expression $[\rho_{gB}(\mathrm{AZ}) = CT + D/T]$. To estimate this resistivity, and the width of the normal state region, the data were fitted to ρ_B for both the expressions of ρ_{gB}, i.e., $\rho_B = (A + BT)/p + \rho_c = A' + B'T$ for the linear expression with $A' = A/p + \rho_c$ and $B' = B/p$ and $\rho_B = CT/p + D/pT + \rho_c = C'T + D'/T + \rho_c$ with $C' = C/p$ and $D' = D/p$ for the AZ expressions. To estimate the width of the normal state region, the upper end of the data was fixed at 270 K and the lower end was varied from 200 K down to 120 K. The rms deviation (rmsd) remained constant (at 0.077% for polycrystalline YBCO, e.g.) till a temperature $\simeq 170$ K, below which the deviation increased rapidly. This lower temperature end of the normal part is $\simeq 2T_c$ for all samples. Both the expressions for ρ_{gB} gave the same rmsd but the value of D' in the $\rho_n(\mathrm{AZ})$ comes out to be very small reflecting the data to follow the linear metallic behavior. We find D' to be six orders of magnitude smaller than C' for both the series (see Table I) giving a nonlinear term $(= D'/T)\ 10^{-10}$ times smaller than the linear contribution $(= C'T)$ at 100 K. This is also reflected by the temperature independence of $d\rho_T/dT$ for $T > T_{\mathrm{onset}}$.

B. Selection of T_c^{mf}

Excess conductivity $\Delta\sigma_{\mathrm{ex}}$ was calculated by subtracting the background conductivity from the measured conductivity $\sigma_T = 1/\rho_T$ as

$$\Delta\sigma_{\mathrm{ex}} = 1/\rho_T - 1/\rho_B \ . \tag{6}$$

TABLE I. Normal state fitted parameters and T_c values for various samples. Both the forms of ρ_{gB} fits with the same rms deviation.

Parameters	YBCO Polycrys.	YBCO film	BSCCO $x=0$	BSCCO $x=0.05$	BSCCO $x=0.20$
ρ_T (275 K) $\mu\Omega$ m	14.33	1.11	60.16	22.20	36.17
T_c ($\rho=0$) K	92.12	86.4	85.7	63.58	50.33
Transition Width K	1	1	4	6	9
$T_c(d\rho_T/dT)$max K	93.5	88.5	88.5	89.0	76.0
Normal Part:					
Fitt. temp. range K	250–168	250–160	260–170	260–150	260–140
A' $\mu\Omega$ m	3.77	0.15	12.36	5.80	8.88
B' $\mu\Omega$ m/K	385.48	35.87	1748.0	591.88	981.34
% rmsd	.07	0.02	0.06	0.06	0.09
C' $\mu\Omega$ m/K	385.20	35.87	1748.0	591.88	981.34
D' (10^{-2} $\mu\Omega$ m K)	0.016	0.200	3.26	2.600	0.055
ρ_c $\mu\Omega$ m	3.76	0.15	12.36	5.80	8.87
% rmsd	0.09	0.03	0.06	0.06	0.09

These high-T_c materials exhibit an anisotropic behavior. The conduction is predominant in the a-b planes at the temperatures away from T_c^{mf}. At temperatures near the T_c^{mf} when correlation length along c axis becomes of the order of interplanar distance d, the excess conductivity shows a cross over from 2D to 3D. The proper selection of T_c^{mf} (mean-field transition temperature) is very important in order to see the dimensionality of the fluctuations. Generally this is taken either as the temperature corresponding to the half of the resistivity value at the T_c onset (T_{c1}) or the temperature (T_{max}) corresponding to the maximum of $d\rho_T/dT$. We have chosen the later criterion. T_{max} also cannot be determined unambiguously: there are errors associated with the flatness of the peak and also with the numerical differentiation of ρ_T to obtain $d\rho_T/dT$. We have tried to vary the T_c^{mf} in small steps around the value of T_{max}. We have plotted $\ln(\Delta\sigma_{ex})$ vs $\ln(\epsilon)$ for various values of T_c^{mf} as shown in Fig. 2. For some value of T_c^{mf} these plots are straight over a wide range of ϵ, indicating thereby that the excess conductivity is trying to obey a power law, $\Delta\sigma_{ex}\simeq\epsilon^{-\nu}$. There is a break in the slope of each one of these plots giving $\nu\simeq 1$ for larger values of ϵ and $\nu\simeq\frac{1}{2}$ for the smaller values. The T_c^{mf} obtained together with the extent over which the exponent ν has the values $\frac{1}{2}$ and 1 are listed in Table II. The width of the plot can be adopted as the criterion for the selection of T_c^{mf}. But a selection of T_c^{mf} on this basis precludes other contributions to $\Delta\sigma_{ex}$ which may have different dependences on ϵ. The other contribution relevant in this region is that due to Maki and Thompson (MT). In zero applied field this is given by[12]

$$\sigma_{MT}=\frac{e^2}{8\hbar d\epsilon(1-\alpha/\delta)}\ln\left[\frac{\delta}{\alpha}\frac{1+\alpha+\sqrt{1+2\alpha}}{1+\delta+\sqrt{1+2\delta}}\right] \quad (7)$$

where $\delta=16\xi_c^2(0)kT\tau_\phi/(\pi\hbar d^2)$. We note that this expression can be simplified. The phase breaking time τ_ϕ has been seen[13] to vary as $\tau_\phi=\tau_0/T$ where τ_0 is a constant. This makes δ independent of T. For the values $\xi_c(0)\simeq 2$ Å, $d\simeq 11.7$ or 30.7 Å and $\tau_0\simeq 10^{-12}$ sec typical of the YBCO and BSCCO systems we obtain $\alpha\gg\delta$ for the entire width of the mean-field region (MFR). Even though α depends upon ϵ, because of the logarithm involved the coefficient within the parenthesis in σ_{MT} becomes a very slowly varying function of T. Further since $\alpha/\delta\gg 1, (1-\alpha/\delta)\simeq-\alpha/\delta$ and the prefactor in Eq. (7) therefore, $e^2/[8\hbar d\epsilon(1-\alpha/\delta)]\simeq -e^2k\tau_0(\pi\hbar^2 d)$ for the values of α and δ defined above. This means σ_{MT} is essentially temperature independent ($\simeq C_{MT}$) or atmost a slowly varying function of T within the entire MFR. This is shown in Fig. 4 for the typical values of the parameters involved.

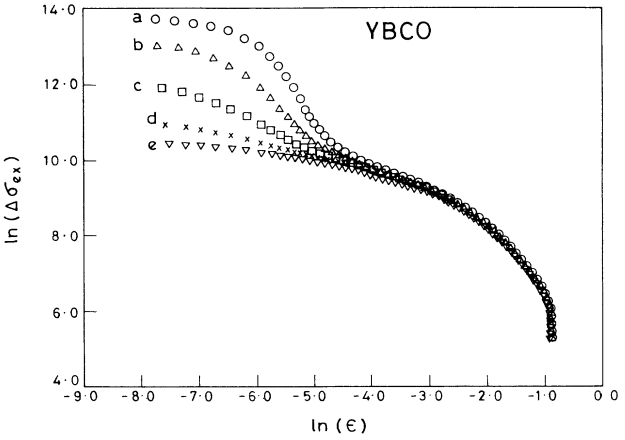

FIG. 2. The plot of $\ln(\Delta\sigma_{ex})$ vs $\ln(\epsilon)$ for YBCO sample for various values of T_c^{mf}: 93.0 K for (a), 93.2 K for (b), 93.4 K for (c), 93.6 K for (d), and 93.8 K for (e).

The excess conductivity which is equal to the sum of σ_{AL} and σ_{MT}, can be written as

$$\Delta\sigma_{ex}=\frac{p}{F}(\sigma_{AL}+\sigma_{MT}) \quad (8)$$

TABLE II. Value of the T_c^{mf} and 2D and/or 3D temperature ranges by choosing T_c^{mf} for the largest 2D and/or 3D widths (Fig. 2), from $1/\Delta\sigma_{ex}$ vs T plots (Fig. 3) and from the Testardi plots (Fig. 5).

Parameters	YBCO Polycrys.	YBCO Film	BSCCO $x=0$	BSCCO $x=0.05$	BSCCO $x=0.20$
Parameters obtained from Fig. 2					
T_c^{mf} K	93.4±0.1	88.4±0.1	88.6±0.1	89.1±0.1	76.0±0.1
3D Temp. range K	94.2–99.8	90–97.3	89.2–90.2	90.8–92	78–79.8
2D Temp. range K	100–105	97.8–105	90.2–100.5	92–100	79.8–96
MFR K	10.8	15	11.3	9.2	18
Critical region K	0.8	1.6	0.6	1.7	2.0
Parameters obtained from Fig. 3					
3D Temp. range K	94–98	90–95			
2D Temp. range K			90.5–100.5	91.6–99	79.5–94.5
T_c^{mf} K	93.4±0.2	88.5±0.2	88.5±0.2	89.0±0.2	76.0±0.2
Parameters obtained from Fig. 5					
3D Temp. range K	94–100	90–98	89–90	91–92	78–80
2D Temp. range K	100–104	98–105	90–101	92–101	80–98
T_c^{mf} K	93.45	88.5	88.54	89.0	76.1

for polycrystalline samples within the Veira model,[8] where

$$1/F=(1-\rho_c/\rho_T)(1-\rho_c/\rho_B)\ . \tag{9}$$

In general F is also a slowly varying function of the temperature and within the same interval, it also will not vary with temperature. Hence over the 2D and the 3D region,

$$\Delta\sigma_{ex}=\frac{p}{F}\left[\frac{C_{AL}}{\epsilon^{\nu}}+C_{MT}\right] \tag{10}$$

with $\nu=1$ or $\frac{1}{2}$ for the respective regions. Thus plots of $Y_2=[\Delta\sigma_{ex}-(p/F)C_{MT}]^{-1}$ vs T in the 2D region and $Y_3=[\Delta\sigma_{ex}-(p/F)C_{MT}]^{-2}$ vs T in the 3D region should give straight lines with the intercept of the lines on the T axis defining the value of T_c^{mf}.

These plots for the undoped BSCCO samples are shown in Fig. 3(a). The values of C_{MT} have been calculated from Eq. (7) for different values of τ_0. Values of p and F have been taken from the nonlinear least-squares fitting procedure described below but their exact values do not appear to have any bearing on the present argument. The curves (a) through (c) in this figure have been drawn for successively decreasing values of τ_0. As can be seen they are curved and appear to stretch over to straight lines with decreasing values of τ_0. Curve (d) is a plot of $1/\Delta\sigma_{ex}$ vs T, i.e., with $C_{MT}=0$ and shows the longest straight portion $\simeq$(90–107 K). This points towards a negligible contribution from the Maki-Thompson process. This temperature range corresponds with the 2D portion of the MFR determined above. Similar behavior was observed in all Y-doped samples. Straight line graphs could only be obtained by assuming vanishing values of C_{MT} in Y_2.

In YBCO samples also Y_3 vs T plots were straight only for $C_{MT}\simeq 0$ [Fig. 3(b)] and here the straight portions matched well with the 3D parts of the MFR. In principle plots of Y_3 vs T for BSCCO over the 3D region and Y_2 vs T for YBCO over the 2D region can also be used to gain information about C_{MT} but their widths were found to be too small for them to be useful.

This procedure puts an upper limit of 10^{-13} sec for τ_0. A value of τ_0 larger than this produces curvatures in the plots that can be detected by the eye. We observe from Fig. 2 that a change of ± 0.1 K in T_c^{mf} changes ν from 0.44 to 0.56. $\Delta\nu\simeq 0.06$ is sufficient to include the MT

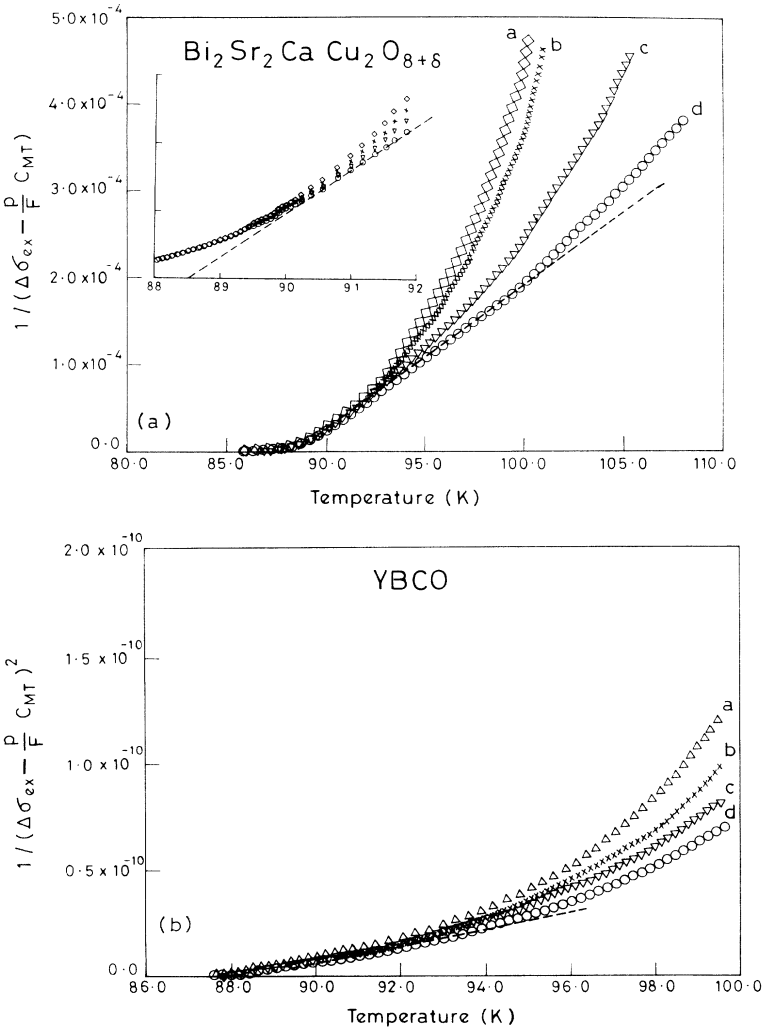

FIG. 3. (a) $(\Delta\sigma_{ex}-pC_{MT}/F)^{-1}$ vs T for the BSCCO sample with C_{MT} decreasing from plots a to d. $C_{MT}=0$ for plot d. Dotted straight line here shows the 2D region in this system. The inset shows the expended view of the region around the intercept which gives T_c^{mf}. (b) $(\Delta\sigma_{ex}-pC_{MT}/F)^{-2}$ vs T for the YBCO sample with C_{MT} decreasing from plots a to d. $C_{MT}=0$ for plot d. Dotted straight line here shows the 3D region in this system.

term due to the slow variation of the latter. T_c^{mf} determined by this method is listed in Table II together with the 2D and 3D regions observed for each sample.

For further analysis, recourse to nonlinear least-squares fitting of the data was taken. $p, \rho_c, \xi_c(0)$ and τ_0 were taken as adjustable parameters. The fittings were performed in the 2D and 3D ranges separately. For the bulk YBCO sample, using $d = 11.7$ Å as the c-axis parameter in the 3D range (i.e., 94–100 K), we get $p = 0.25$, $\rho_c = 3.5\ \mu\Omega$ m, $\xi_c(0) = 1.98$ Å and $\tau_0 = 2\times10^{-26}$ sec. The fit is of good quality as rmsd is low (0.13%) as well as from the point of view that the parameters obtained (except T_c^{mf}) have reliable values. The same procedure for the film samples gave $\rho_c = 0.17\ \mu\Omega$ m and $p = 0.76$. An increase in p and decrease in ρ_c is expected as the grains in the film are larger and aligned better than in the bulk YBCO. The T_c^{mf} was allowed to vary within small limits around T_{max}. However the value of τ_0 obtained $\simeq 10^{-26}$ sec implies again a near absence of the MT contribution. Similar results are obtained from the fitting in the 2D region or from σ_{LD} when both the regions are combined together. (We obtain fits of inferior quality when σ_{LD} is used as compared to the fits over the two separate regions and feel that the expression of σ_{LD} does not change over in the dimensionality as fast as the data requires.) Further a larger value of τ_0 deteriorates the fits drastically. We find the fit quality to remain uneffected for $\tau_0 \lesssim 10^{-12}$ sec and the rmsd to jump abruptly to 1% or more for larger values of τ_0. Results are found to be similar for all five samples with $\tau_0 \simeq 2\times10^{-12}$ sec (corresponding to $\tau_\phi \simeq 2\times10^{-14}$ sec at 100 K) as the maximum value of τ_0 that can be tolerated without any increase in the rmsd value. (In general the BSCCO samples require smaller values of τ_0 in fits over the 2D than those over the 3D regions.) The fits are shown in Fig. 4 along with the individual contributions. The values of the parameters obtained are listed in Table III.

Testardi *et al.*[10] have devised a method to determine ν for the low-T_c materials. The method did not require any prior knowledge of T_c^{mf}. Bhatia *et al.*[20] used this method to show the MFR in TBCCO 2:2:1:2 system to be predominantly 2D in nature. To use this method for the present case, we combine Eq. (6) with (8)

$$\frac{1}{\rho_T} - \frac{1}{\rho_B} = \Delta\sigma_{ex} = \frac{p}{F}(\sigma_{AL} + \sigma_{MT}) \tag{11}$$

and differentiate both sides with respect to T to get

$$-\left[\frac{1}{\rho_T^2}\frac{d\rho_T}{dT} - \frac{1}{\rho_B^2}\frac{d\rho_B}{dT}\right] = -\frac{p}{F^2}\frac{dF}{dT}(\sigma_{AL}+\sigma_{MT}) + \frac{p}{F}\frac{d}{dT}(\sigma_{AL}+\sigma_{MT})$$

Since F and C_{MT} are slowly varying functions of temperature $dF/dT \simeq dC_{MT}/dT \simeq 0$, and therefore,

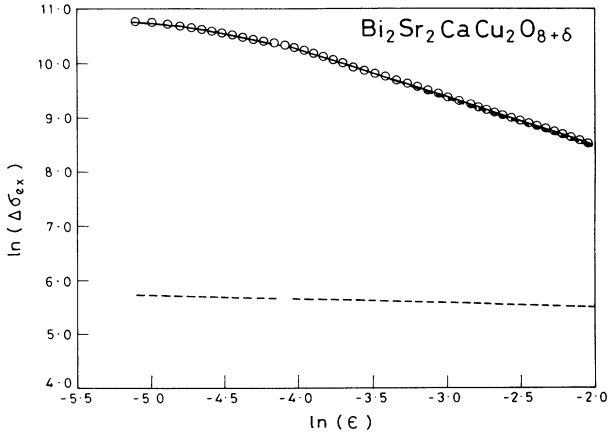

FIG. 4. Experimental excess conductivity data (circles) are shown with fitted theoretical expression (solid curve) in the 2D and 3D regions for the BSCCO samples. MT contribution for $\tau_\phi \simeq 10^{-15}$ sec is shown by the dotted line.

TABLE III. Values of the various fitted parameters.

Parameters	YBCO Polycrys.	YBCO film	BSCCO $x=0$	BSCCO $x=0.05$	BSCCO $x=0.20$
Excess conductivity fitted					
T_c^{mf} K	93.45	88.45	88.6	89.1	76.0
3D temp. range K	94–100	90–97	89.2–90.2	90.7–91.8	78–79.8
2D temp. range K	100.5–104	98–103	90.3–101	91.9–100.5	80–95.7
MFR K	10	13	11.7	10.7	17.6
p	0.25	0.76	0.26	0.25	0.22
$\xi_c(0)$ Å	1.98	1.67	1.68	2.30	3.60
$\xi_c(0)$ Å from T_{cr}	1.58	1.87	2.07	2.66	3.46
τ_ϕ (3D) sec at 100 K	2.2×10^{-24}	3.2×10^{-22}	1.8×10^{-26}	1.5×10^{-25}	4.9×10^{-26}
% rmsd in 3D	0.15	0.18	0.14	0.10	0.09
τ_ϕ (2D) sec at 100 K	4.1×10^{-28}	1.1×10^{-27}	2.8×10^{-28}	2.8×10^{-26}	8.4×10^{-32}
% rmsd in 2D	0.18	0.14	0.15	0.09	0.05
$\rho_c\ \mu\Omega$ m	3.53	0.17	3.48	6.62	3.85
T_{cr}/T_c	1.07	1.09	1.02	1.03	1.04
Critical region K	0.55	1.55	0.6	1.63	2.07
Slope 3 above MFR K	110–140	112–138	135–148	111–138	110–138

$$-\left[\frac{1}{\rho_T^2}\frac{d\rho_T}{dT}-\frac{1}{\rho_B^2}\frac{d\rho_B}{dT}\right]=\frac{p\nu}{FT_c^{\rm mf}}\frac{C_{\rm AL}}{\epsilon^{\nu+1}}$$
$$=\frac{\nu}{T_c^{\rm mf}}\left\{\frac{F}{pC_{\rm AL}}\right\}^{1/\nu}\times\left[\Delta\sigma_{\rm ex}-\frac{pC_{\rm MT}}{F}\right]^{1+1/\nu}$$

after using Eq. (10) to eliminate ϵ. Further, using Eq. (6) the right-hand side (RHS) becomes

$$=\frac{\nu}{T_c}\left\{\frac{F}{pC_{\rm AL}}\right\}^{1/\nu}\left[\left\{\frac{1}{\rho_T}-\frac{1}{\rho_B}\right\}-\frac{pC_{\rm MT}}{F}\right]^{1+1/\nu}$$
$$=\frac{\nu}{T_c}\left\{\frac{F}{pC_{\rm Al}}\right\}^{1/\nu}X$$

where X represents the quantity in the square brackets. Thus a plot of $\ln(Y)$ where

$$Y=-\left[\frac{1}{\rho_T^2}\frac{d\rho_T}{dT}-\frac{1}{\rho_B^2}\frac{d\rho_B}{dT}\right]$$

against $\ln(X)$ will have a slope $1+1/\nu=2$ in the 2D region and 3 in 3D region and an intercept

$$=\ln\left[\frac{\nu}{T_c}\left\{\frac{F}{pC_{\rm AL}}\right\}^{1/\nu}\right].$$

$d\rho_T/dT$ was obtained by numerically differentiating the data as mentioned above. $d\rho_B/dT=B'$, its value obtained from the high-temperature part of the fit, i.e., $T>2T_c$ was used. Once again straight line graphs could only be obtained with $C_{\rm MT}\simeq 0$ for all the samples studied. The plots are shown in Fig. 5. 2D and 3D temperature ranges obtained are listed in Table II along with the values of $T_c^{\rm mf}$ calculated from the intercept. The agreement is seen to be excellent. In YBCO samples a change of slope from 3 to 2 is clearly discernible, whereas in BSCCO this is masked by the larger width of the 2D region.

Recently another method—the logarithmic derivative method—has been proposed by Pureur *et al.*[11] This method also does not require any prior knowledge of $T_c^{\rm mf}$ and is especially useful if a power law is the only function by which the conductivity varies. Thus if $C_{\rm MT}$ is actually negligible as the above analysis suggests then Eq. (10) gives

$$\frac{d}{dT}(\ln\Delta\sigma_{\rm ex})=-\frac{\nu}{\epsilon}\frac{1}{T_c^{\rm mf}}=\frac{\nu}{T-T_c^{\rm mf}}\ . \qquad (12)$$

Then a plot of

$$\chi=\left[-\frac{d}{dT}\ln\Delta\sigma_{\rm ex}\right]^{-1}$$

against T will yield ν from the slope and $T_c^{\rm mf}$ from the intercept. Additional advantage of these plots is that unlike in Eq. (11) F here does not contribute to RHS. Equation (12) will therefore, give identical plots for polycrystalline as well as single crystals.

Figures 6(a) and 6(b) display these plots for YBCO and BSCCO samples, respectively. All BSCCO samples are unambigous in displaying long straight portions corresponding to $\nu\simeq 1$. Although considerable scatter is present in the derivatives, they lead to only small errors in the determinations of ν here. The limits of the 2D region and $T_c^{\rm mf}$ determined here match favorably with the above results. The 3D region gives considerable error in $T_c^{\rm mf}$ due to its short length. The YBCO plots are not as unambigous. Although straight lines with $\nu=1/2$ and 1 can be identified, the graph appears to consist of many short segments each with a specific ν.

Thus we find that four different methods give identical values of $T_c^{\rm mf}$ for each sample and the values of the exponents remain $\frac{1}{2}$ and 1. The extent over which these exponents are found defines the mean-field region. This is found to extend from $-5.0\le\ln(\epsilon)\le -2.0$ for all the five samples. For both the YBCO samples, the MFR is dom-

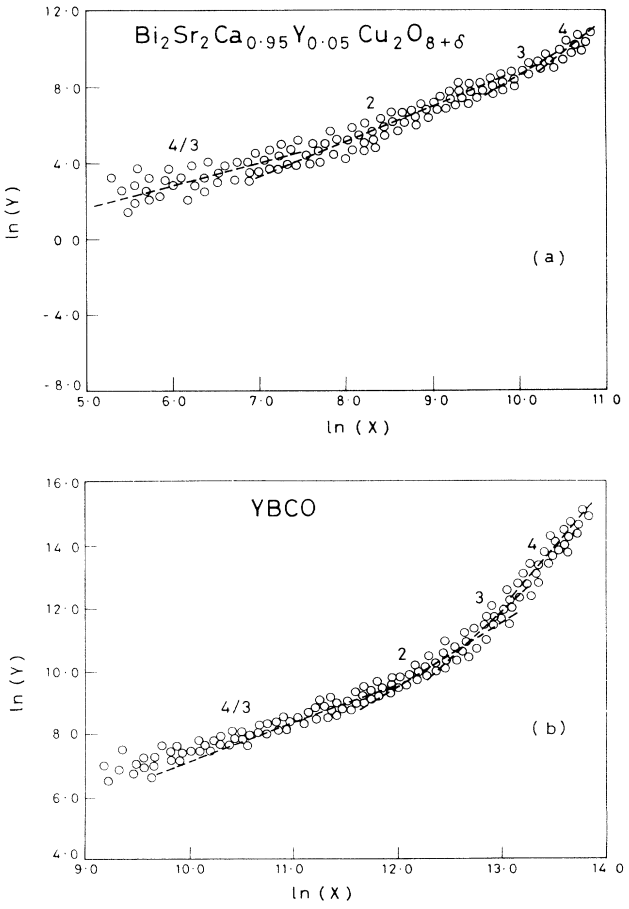

FIG. 5. (a) Testardi plots using derivative method for the BSCCO sample showing the slopes 2 and 3 for the 2D and 3D regions. Slope 4 at the low temperature side (large X) and $\frac{4}{3}$ at the higher-temperature side show the presence of the critical region and short-wavelength fluctuations region, respectively. (b) Testardi plot for YBCO. Critical and short-wavelength fluctuations regions are wider compared to BSCCO.

inated by 3D region with a cross over from 3D to 2D occurring at $\ln(\epsilon)\simeq -3.0$. This gives the cross over temperature $T_{cr}=1.05T_c$. In all the BSCCO samples 2D behavior was seen over most of the MFR. For Y free samples the dimensionality cross over occurred at $\ln(\epsilon)\simeq -4.0$. With Y doping the cross over temperature shifted to higher (reduced) temperatures together with a slight increase in the width of the 3D region. Below the MFR, i.e., $\ln(\epsilon)\leq -5.0$ the systems pass into the critical regions. In YBCO the exponents were seen to change from $\frac{1}{2}$ to $\frac{2}{3}$ and then to $\frac{1}{3}$ [Fig. 7(a)]. The critical region was found to extend to around 0.5 K above T_c^{mf} in both the samples. These values of the exponents follow the predictions of Lobb[21] that the phase transition in this system is analogous to 3D-XY model.

In the BSCCO samples we did observe the exponent to change to $\frac{1}{3}$ and reduce further as the temperature was lowered [Fig. 7(b)]. Unlike the YBCO system the exponent $\frac{2}{3}$ was not found immediately below the MFR. The critical region increased in width from 0.4 K for $x=0$ to 1 K for $x=0.20$ samples. In 2D-XY model,

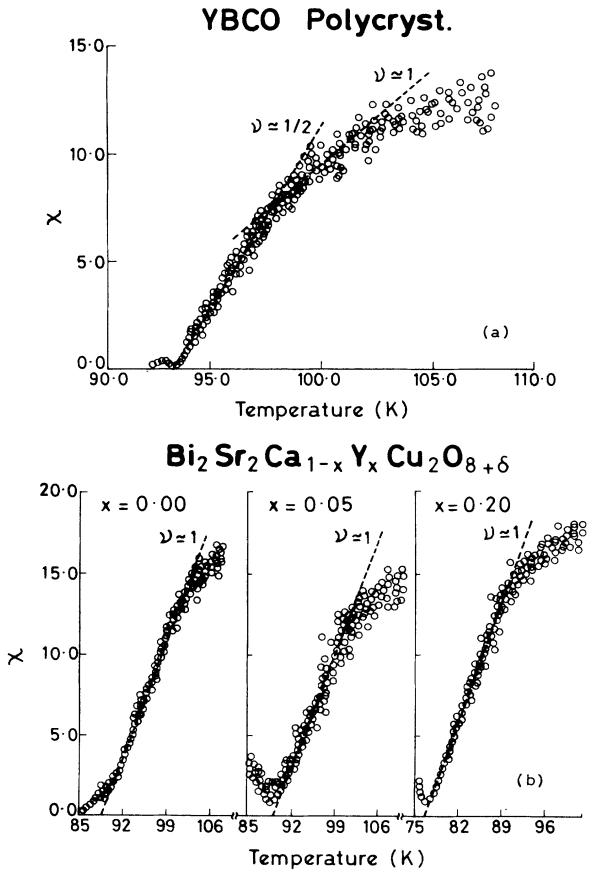

FIG. 6. (a) Logarithmic derivative plot for YBCO. Dotted lines show the 3D and 2D regions for $\nu\simeq\frac{1}{2}$ and 1, respectively. (b) Logarithmic derivative plots for BSCCO samples for $x=0.0$, 0.05, and 0.20. A significantly wide 2D region with $\nu\simeq 1$ has been observed in all the samples showing the absence of fractional dimensionality.

Luther and Scalapino[22] have found the exponent to be $1/\sqrt{8}$ ($=0.35$) below MFR and decrease further at lower temperatures. Our values of the exponent thus agree with this prediction. A change of behavior from 3D-XY like to 2D-XY like in BSCCO is expected as the interlayer spacing in BSCCO has increased to three times its value in YBCO.

We have also observed deviation in the slope from the 2D behavior outside the upper end of the MFR. Similar departure from the 3D behavior has been observed in the amorphous superconductors by Johnson, Tsuei, and Chaudhari,[23] and in high-T_c materials by Frietas, Tsuei, and Plaskett.[3] They tried to interpret this in the YBCO system by introducing a cut off to remove the short-wavelength fluctuations, for which the GL theory did not apply. Recently Reggiani, Vaglio, and Varlamov[24] have explained the fluctuations in a wide temperature range by taking into consideration all the boson frequencies and momenta in the fluctuations and have shown the excess conductivity in the higher-temperature range ($\epsilon\rightarrow\infty$) to vary as $\Delta\sigma_{ex}\simeq 1/\epsilon^3$. We have observed the exponent to be 3 in a wide temperature range in the YBCO bulk and thin-film samples [Fig. 7(a)]. For the bulk sample the range is 114–150 K and for the film 113–140 K. 113 K corresponds to the temperature where the MFR ends while the upper end of this range (140 or 150 K) comes close to the temperature down to which the background conductivity part was fitted. However the behavior is quite different in BSCCO. The exponent ν varies continuously from 3 to 8 in this region. It has a value 3 in a narrow ϵ range only, and this range increases with increasing Y concentration. 3 is the maximum value predicted by Reggiani, Vaglio, and Varlamov[24] for ν. Discrepancy here or the fortuous agreement in YBCO can be traced to two factors. The magnitude of $\Delta\sigma_{ex}$ in YBCO is quite high ($\simeq 10^4\ \Omega^{-1}\mathrm{m}^{-1}$) and that in BSCCO low ($\simeq 10^2\ \Omega^{-1}\mathrm{m}^{-1}$) within the MFR. Consequently errors associated with the extraction of $\Delta\sigma_{ex}$ from ρ_T will have more significant influence in BSCCO than in YBCO. MT contribution as predicted by Eq. (7) is a slowly varying function of ϵ and therefore has significant values in this region of ϵ. In fact the calculated value of σ_{MT} is larger than $\Delta\sigma_{ex}$ for BSCCO for τ_0 around 10^{-13} sec, which is the value that gives vanishing contribution in the MFR. Further this term has been derived for $\epsilon\leq 1$ and may not be valid in this range of ϵ. Also it appears that σ_{MT} must be falling off more rapidly in YBCO than in BSCCO. These results are at variance with the conclusions of Balestrino *et al.*[25] on epitaxial films of BSCCO. They observed smaller values of the exponent ($\nu<3$) over an ϵ range equivalent to that investigated in the present case.

The values of the exponent are corroborated by Testardi plots also. Thus in Fig. 5(a) the slope increases to 4 for $\ln(X)\geq 13$ and decreases to $\frac{4}{3}$ on the other side of the plot, i.e., for $\ln(X)\leq 11$. These correspond to $\nu=\frac{1}{3}$ near T_c^{mf} and $\nu=3$ above the 2D region. However such clear slopes were not seen for BSCCO samples, although general trends with slopes 4 on higher abscissa and $\frac{4}{3}$ on lower side could be traced [Fig. 5(b)]. Errors associated

with numerical differentiation lead to large scatter of the data.

Our data are not able to support the contention of Pureur *et al.*[11] about the presence of fractals from the logarithmic plots. Their argument is based on the observation of a region of $\nu_2=0.85\pm0.09$ bounded by regions of $\nu_3=0.51\pm0.06$ and $\nu_1=1.32\pm0.15$. The values ν_1 and ν_2 correspond to (fractional) dimensions $\frac{4}{3}$ and $\frac{7}{3}$ $(=1+\frac{4}{3})$ of Gaussian fluctuations in fractal topology. Our plots do not show discrete regions with these values of ν_1 and ν_2. As mentioned above, the exponent ν changes almost continuously from 0.5 to 1.0 in the 3D to 2D change over. It is difficult to identify any finite length of the plots with discrete values 0.85 and 1.33 of the exponent. Further the scatter in these plots is more than in the Testardi plots and it is difficult to identify the $\nu=3$ exponent.

We have further noted that the fractional values of the exponent result from the incomplete subtraction of the normal resistivity. If the intercept A_g in ρ_n is increased, this leads to underestimation of ρ_n and therefore, the value of $\Delta\sigma_{ex}$ increases and that of ν decreases. Reverse is true when A_g is decreased. A $\pm10\%$ change in A_g changes ν from 0.8 to 1.2.

Both Ausloos, Clippe, and Laurent[26] and Pureur *et al.*[11] have numerically differentiated their data of excess resistivity and excess conductivity, respectively, and display very smooth curves. Our data, on the other hand, shows considerable scatter. It is hard to imagine even a good quality ρ_T vs T data giving no scatter upon differentiation. So also is the abrupt change of dimensionality from $\frac{4}{3}$ to $\frac{7}{3}$ as seen by Pureur *et al.*[11]

IV. CONCLUSIONS

With the proper selection of the T_c^{mf} we have found that for both the systems YBCO as well as BSCCO, the dimensionality of the fluctuations show a cross over from 2D to 3D behavior within the MFR as suggested by Lawrence and Doniach. We also find the critical exponent values to be $\frac{2}{3}$ and $\frac{1}{3}$ in the critical region as proposed by Lobb and observed by Veira *et al.* Pair-breaking effects are found to be strong in both systems with a negligible contribution of the MT term.

The alternative methods Figs. 3, 5, and 6 used here

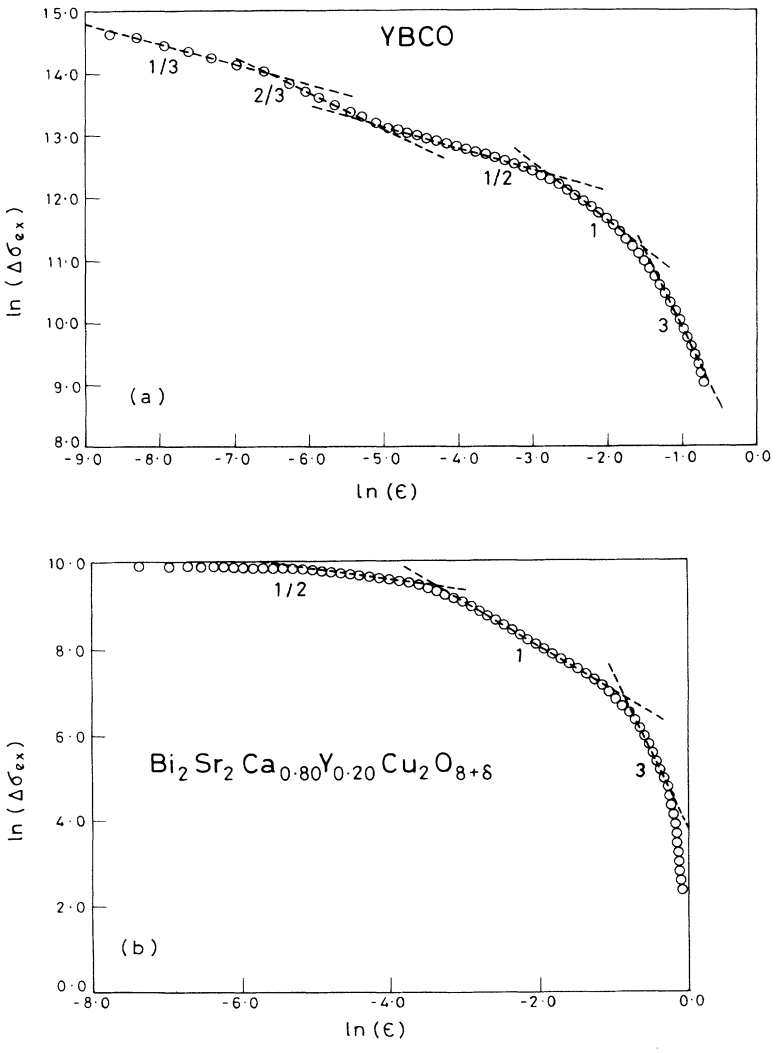

FIG. 7. (a) Various values of the exponents for the YBCO thin-film sample are shown. Within the MFR the exponent changes from 1 to $\frac{1}{2}$. The value $\frac{2}{3}$ and $\frac{1}{3}$ have been observed in the critical region. Slope 3 has been observed at the high-temperature side of the MFR as predicted by Reggiani *et al.* (b) $\ln(\Delta\sigma_{ex})$ vs $\ln(\epsilon)$ plot for BSCCO. Slopes 1 and $\frac{1}{2}$ have been observed within the MFR. Slope 3 has been observed above MFR in a temperature range narrower compared to YBCO.

have limited utility. In the Testardi and the logarithm plots the precision of ν is determined by the accuracy of calculating $d\rho_T/dT$. Large errors in determination of this derivative can easily mask a region as is obvious from the absence of the critical region in the BSCCO in Fig. 5(b) although this region is clearly present in Fig. 4. These methods at best can be considered as supplementary to the nonlinear least-squares fitting procedure. However the logarithmic plots show clearly the regions with exponent very close to 1.0, implying the absence of the MT contribution. This is the region where this contribution is expected to show its maximum effect. These plots also do not corroborate a fractional dimension for the fluctuations.

[1]L. G. Aslamazov and A. I. Larkin, Phys. Letts. **26A**, 238 (1968).

[2]J. Lawrence and S. Doniach, in *Proceedings of the Twelfth International Conference on Low Temperature Physics, Kyoto 1970,* edited by E. Kanda (Academic, Kyoto, Japan, 1971), p. 361.

[3]P. P. Freitas, C. C. Tsuei, and T. S. Plaskett, Phys. Rev. B **36**, 833 (1987).

[4]B. Oh, K. Char, A. D. Kent, M. Naito, and M. R. Beasley, T. H. Geballe, R. H. Hammond, and A. Kapitulnik, Phys. Rev. B **37**, 7861 (1988).

[5]S. J. Hagen, Z. Z. Wang, and N. P. Ong, Phys. Rev. B **38**, 7137 (1988).

[6]T. A. Friedmann, J. P. Rice, J. Giapintzakis, and D. M. Ginsberg, Phys. Rev. B **39**, 4258 (1989).

[7]K. Maki, Prog. Theor. Phys. **39**, 897 (1968), **40**, 193 (1968). R. S. Thompson, Phys. Rev. B **1**, 327 (1970).

[8]J. A. Veira and F. Vidal, Physica C **159**, 468 (1989).

[9]S. N. Bhatia, C. P. Dhard, I. K. Gopalakrishnan, P. V. P. S. S. Sastry, J. V. Yakhmi, and R. M. Iyer, Physica C **185–189**, 1845 (1991).

[10]L. R. Testardi, W. A. Reed, P. C. Hohenberg, W. H. Hammerle, and G. F. Brennert, Phys. Rev. **181**, 800 (1969).

[11]P. Pureur, R. Menegotto Costa, P. Rodrigues, J. Schaf, and J. V. Kunzler, Phys. Rev. B **47**, 11 420 (1993).

[12]S. Hikami and A. I. Larkin, Mod. Phys. Lett. B **2**, 693 (1988).

[13]Y. Matsuda, T. Hirai, and S. Komiyama, Solid State Commun. **68**, 103 (1988); Y. Matsuda, T. Hirai, S. Komiyama, T. Terashima, Y. Bando, K. Iijima, K. Yamamoto, and K. Hirata, Phys. Rev. B **40**, 5176 (1989).

[14]M. Hikita and M. Suzuki, Phys. Rev. B **39**, 4756 (1989); **41**, 834 (1990).

[15]Ju-Jin Kim, J. Kim, H. J. Shin, H. J. Lee, and J. K. Ku, Solid State Commun. **75**, 921 (1990).

[16]J. A. Veira and F. Vidal, Phys. Rev. B **42**, 8748 (1990).

[17]K. Char and A. Kapitulnik, Z. Phys. B **72**, 253 (1988).

[18]P. Clippe, Ch. Laurent, S. K. Patapis, and M. Ausloos, Phys. Rev. B **42**, 8611 (1990).

[19]N. Mori, J. A. Wilson, and H. Ozaki, Phys. Rev. B **45**, 10 633 (1992).

[20]S. N. Bhatia, R. Walia, I. K. Gopalakrishnan, P. V. P. S. S. Sastry, J. V. Yakhmi, and R. M. Iyer, Solid State Commun. **75**, 415 (1990).

[21]C. J. Lobb, Phys. Rev. B **36**, 3930 (1987).

[22]A. Luther and D. J. Scalapino, Phys. Rev. B **16**, 1153 (1977).

[23]W. L. Johnson, C. C. Tsuei, and P. Chaudhari, Phys. Rev. B **17**, 2884 (1978).

[24]L. Reggiani, R. Vaglio, and A. A. Varlamov, Phys. Rev. B **44**, 9541 (1991).

[25]G. Balestrino, M. Marinelli, E. Milani, L. Reggiani, R. Vaglio, and A. A. Varlamov, Phys. Rev. B **46**, 14 919 (1992).

[26]M. Ausloos, P. Clippe, and Ch. Laurent, Phys. Rev. B **41**, 9506 (1990).